

The Physics of Chromospheric Plasmas
ASP Conference Series, Vol. 368, 2007
Petr Heinzel, Ivan Dorotovič and Robert J. Rutten, eds.

Multi-wavelength Analysis of a Quiet Solar Region

G. Tsiropoula¹, K. Tziotziou¹, J. Giannikakis¹, P. Young², U. Schühle³
 and P. Heinzel⁴

¹*Institute for Space Applications and Remote Sensing, Athens, Greece*

²*CCLRC Rutherford Appleton Laboratory, United Kingdom*

³*MPI für Sonnensystemforschung, Katlenburg-Lindau, Germany*

⁴*Astronomical Institute AS, Ondřejov, Czech Republic*

Abstract. We present observations of a solar quiet region obtained by the ground-based Dutch Open Telescope (DOT), and by instruments on the space-craft SOHO and TRACE. The observations were obtained during a coordinated observing campaign on October 2005. The aim of this work is to present the rich diversity of fine-scale structures that are found at the network boundaries and their appearance in different instruments and different spectral lines that span the photosphere to the corona. Detailed studies of these structures are crucial to understanding their dynamics in different solar layers, as well as the role such structures play in the mass balance and heating of the solar atmosphere.

1. Introduction

In the quiet regions of the solar surface the magnetic field is mainly concentrated at the boundaries of the network cells. Over the past decade, apart from the well-known mottles and spicules, several other structures residing at the network boundaries such as explosive events, blinkers, network flares, upflow events have been mentioned in the literature. However, their interpretation, inter-relationship and their relation to the underlying photospheric magnetic concentrations remain ambiguous, because the same feature has a different appearance when observed in different spectral lines and by different instruments. For most of the events mentioned above magnetic reconnection is suggested as the driving mechanism. This is not surprising, since it is now well established from investigations of high resolution magnetograms, that new bipolar elements emerge continuously inside the cell interiors and are, subsequently, swept at the network boundaries by the supergranular flow (Wang et al. 2006; Schrijver et al. 1997). Interactions of the magnetic fields have as a result either the enhancement of the flux concentration in the case of same polarities or its cancellation in the case of opposite polarities. Observations support the idea that flux cancellation most likely invokes magnetic reconnection. In this context, the study and comprehension of the dynamical behaviour of the different fine-scale structures is crucial to the understanding of the dynamics of the solar atmosphere.

In this work we present observations of a solar quiet region and some of the properties of several different structures appearing at the network boundaries and observed in different wavelengths by the different instruments involved in a coordinated campaign.

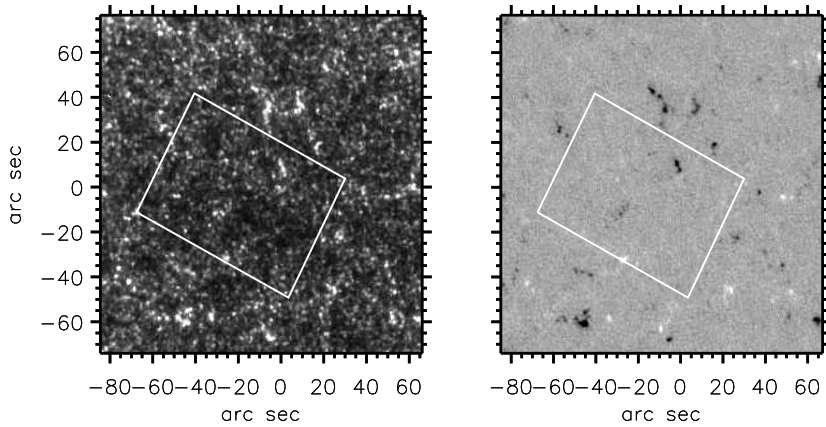


Figure 1. *Left:* CIV TRACE image. *Right:* MDI magnetogram. The white rectangle inside the images marks the DOT's field-of-view.

2. Observations and Data Reduction

In October 2005 we ran a 12 days observational campaign. The aim of that campaign was the collection of multi-wavelength observations both from the ground and space that could be used for the study of the dynamical behaviour of mottles/spicules and other fine structures, observed in different layers of the solar atmosphere.

Three ground-based telescopes were involved in that campaign: DOT on La Palma, THEMIS on Tenerife and SOLIS at Kitt Peak. From space telescopes two spacecraft were involved: SOHO (with CDS, SUMER, and MDI) and TRACE.

The analysed data were obtained on October 14 and consist of time sequences of observations of a quiet region found at the solar disk center recorded by different instruments. Sequences recorded by the DOT were obtained between 10:15:43 – 10:30:42 UT and consist of 26 speckle reconstructed images taken simultaneously at a cadence of 35 s with a pixel size of $0.071''$ in 5 wavelengths along the H α line profile (i.e. at -0.7 \AA , -0.35 \AA , line centre, 0.35 \AA and 0.7 \AA), in the G band with a 10 \AA filter, in the CaIIH line taken with a narrow band filter and in the blue and red continuum. TRACE obtained high cadence filter images at 1550 \AA , 1600 \AA and 1700 \AA . SUMER obtained raster scans and sit-and-stare observations from 8:15 to 10:30 UT. CDS obtained sit-and-stare observations from 6:44 to 10:46 UT and six $154'' \times 240''$ raster scans (each one having a duration of 30 min) from 10:46 to 13:52 UT. Both SOHO instruments (i.e., CDS and SUMER) observed in several spectral lines spanning the upper solar atmosphere. Using the standard software the raw measurements were corrected for flat field, cosmic rays and other instrumental effects. A single Gaussian with a linear background and Poisson statistics were used for fitting each spectral line profile. MDI obtained high cadence images at its high resolution mode.

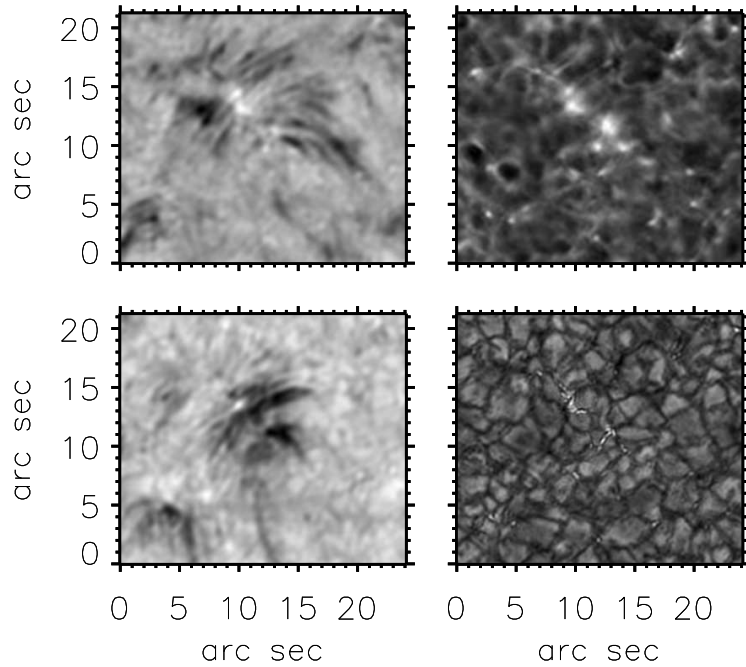


Figure 2. DOT images of a rosette region. *Left:* $H\alpha - 0.7 \text{ \AA}$ (*first row*), $H\alpha + 0.7 \text{ \AA}$ (*second row*). *Right:* Ca II H (*first row*), G band (*second row*).

Extensive work went into collecting, scaling and co-aligning the various data sets to a common coordinate system (see Fig. 1 showing the coalignment of TRACE, MDI, and DOT images).

3. Analysis and Results

3.1. DOT observations

DOT's field-of-view (FOV) is $80''$ in the X direction and $63''$ in the Y direction. For the present study we selected a smaller region which contains a rosette with several mottles pointing to a common center (see Fig. 2) and is found at the middle upper part of the DOT's FOV. In the G-band image (Fig. 2, *right, second row*) isolated bright points show up in the regions of strong magnetic field as can be seen in the MDI image. These seem to be passively advected with the general granular flow field in the intergranular lanes. While we have not conducted an exhaustive study of bright point lifetimes we find that bright points can be visible from some minutes up to almost the entire length of the time series. In the contemporaneous Ca II H images (Fig. 2, *right, first row*) bright points are less sharp due to strong scattering in this line and possibly due to increasing flux tube with height. Reversed granulation caused by convection reversal is obvious in this image.

In the $H\alpha - 0.7 \text{ \AA}$ (Fig. 2, *left, first row*) the dark streaks are part of the elongated $H\alpha$ mottles seen better at $H\alpha$ line center. Some mottle endings appear

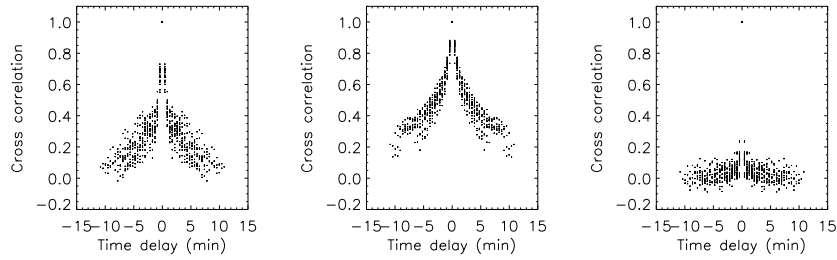


Figure 3. Cross correlation function vs time for *Left*: the intensity at $\text{H}\alpha - 0.7 \text{\AA}$, *Middle*: the intensity at $\text{H}\alpha$ line center. *Right*: the velocity at $\text{H}\alpha - 0.7 \text{\AA}$.

extra dark in the blue wing image through Doppler blueshift. Near the mottle endings one can see bright points. These are sharper in the G-band but stand out much clearer in the $\text{H}\alpha$ wing. Thus $\text{H}\alpha$ wing represents a promising proxy magnetometer to locate and track isolated intermittent magnetic elements. This is because the $\text{H}\alpha$ wing has a strong photospheric contribution, as it is shown by Leenaarts et al. (2006) who arrived to this conclusion by using radiative transfer calculations and convective simulations. In the $\text{H}\alpha + 0.7 \text{\AA}$ (Fig. 2, *left, second row*) dark streaks around the rosette's center are signatures of redshifts. Blueshifts in the outer endings and redshifts in the inner endings of mottles provide evidence for the presence of bi-directional flows along these structures.

An important parameter for the study of the dynamics of mottles is their velocity. For its determination, when filtergrams at two wavelengths of equal intensity at the blue and the red side of the line are available, a technique based on the subtraction of images can be used. In this technique, by using the well known representation of the line intensity profile and assuming a Gaussian wavelength dependence of the optical thickness, we can define the parameter DS:

$$DS = \frac{\Delta I}{\Sigma I - 2I_{0\lambda}}, \quad (1)$$

where $\Delta I = I(-\Delta\lambda) - I(+\Delta\lambda)$, $\Sigma I = I(-\Delta\lambda) + I(+\Delta\lambda)$ and $I_0(\Delta\lambda)$ is the reference profile emitted by the background. DS is called Doppler signal, has the same sign as the velocity and can be used for a qualitative description of the velocity field (for a description of the method see Tsiropoula 2000). When an optical depth less than one is assumed then quantitative values of the velocity can be obtained from the relation:

$$v = \frac{\Delta\lambda_D^2}{4\Delta\lambda} \frac{c}{\lambda} \ln \frac{1 + DS}{1 - DS}, \quad (2)$$

since in that case the velocity depends only on DS (obtained from the observations) and the Doppler width, $\Delta\lambda_D$ (obtained from the literature). By using these relations we have constructed 2-D intensity and velocity images for the whole time series. We found out that it is difficult to follow each one mottle for more than two or three frames and that the general appearance of the region

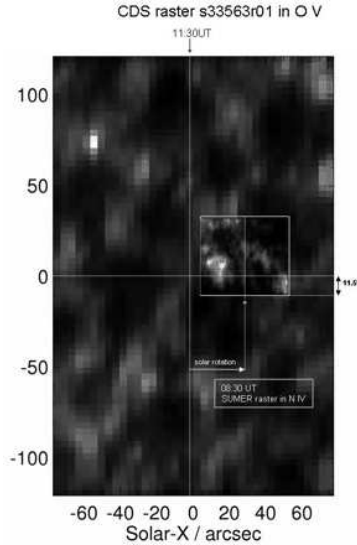


Figure 4. CDS raster image obtained at the O V 629.7 Å line with an overplotted SUMER image at Ne VIII 770 Å.

seems to change quite rapidly with time. For a quantitative estimate of the temporal changes we computed the value of the cross correlation (CC) function over the 2-D FOV both for the intensity and velocity. Figure 3 shows the intensity CC curve at H α – 0.7 Å (*left*) and H α line center (*middle*) and the velocity CC curve at H α ± 0.7 Å (*right*). The decay of the CC curve is a measure of the lifetime of the structures. The e-folding time for the left curve is found equal to 2 min, the middle curve equal to 5 min and the right curve is of the order of the cadence.

3.2. CDS and SUMER observations

In Fig. 4 we show the CDS raster image obtained in the O V 629.7 Å line with the SUMER image at Ne VIII 770 Å overplotted. Although there is a time difference of 3 hours between the two images the network is constant enough to allowed the coalignment of the two images. In CDS intensity maps several brightenings are observed which are called blinkers (Harrison et al. 1999). These events are best observed in transition region lines and show an intensity increase of 60 - 80%. Most of them have a repetitive character and reappear at the same position several times.

In Fig. 5 (*left, up*) we show an integrated (over the spectral line with the background included) intensity image in the Ne VIII 770 Å line produced by sit-and-stare observations of a network region. The image is produced by binning over 6 spectra in order to improve the signal-to-noise ratio. The Doppler shift map was derived by applying a single Gaussian fitting (Fig. 5, *left, bottom*). The Doppler shift map and the spectral line profiles were visually inspected for any non-Gaussian profiles with enhancements in both the blue and red wings that are the main characteristics of the presence of bi-directional jets. Large numbers of such profiles were found at the network boundaries (Fig. 5, *right*).

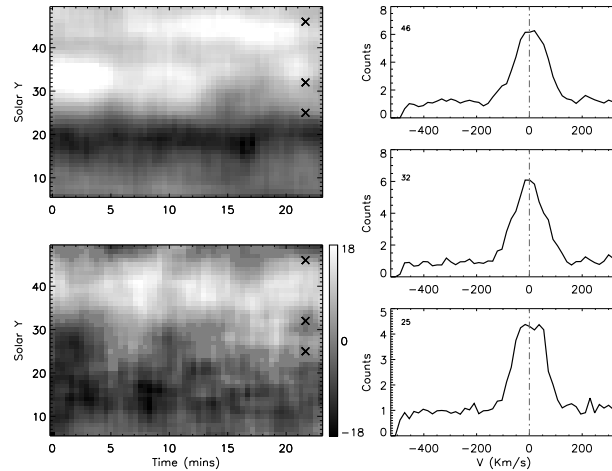


Figure 5. SUMER sit-and-stare observations in the Ne VIII line. *Left:* intensities (*up*), Doppler velocities (*bottom*) (network boundaries are bright in the intensity image). *Right:* non-Gaussian profiles in the positions marked by “x” inside the images in the left.

4. Conclusions

In this work we present observations of a quiet solar region obtained by different instruments in different spectral lines. Network boundaries are found to be the locus of several structures which have different appearances when observed by different instruments e.g., blinkers (when observed with CDS), mottles (when observed with DOT), jets (when observed with SUMER). Their interrelationship is to be further explored.

Regarding flows no-clear pattern is found in blinkers, while bi-directional flows are found in jets. In dark mottles downward velocities are found at their footpoints and upwards velocities at their upper parts and very fast changes in their appearance.

The network shows a remarkable constancy when observed in low resolution images. However when seen in high resolution images several fine structures are observed which change so fast that it is very hard to follow.

Acknowledgments. K. Tziotziou acknowledges support by Marie Curie European Reintegration Grant MERG-CT-2004-021626. This work has been partly supported by a Greek-Czech programme of cooperation.

References

Harrison, A., Lang, J., Brooks, D.H., & Innes, D.E. 1999, A&A, 351, 1115
 Leenarts, J., Rutten, R.J., Sütterlin, P., Carlsson, M., & Uitenbroek H. 2006, A&A, 449, 1209
 Schrijver, C.J., Title, A.M., Van Ballegooijen, A.A., Hagenaar, H.J., & Shine, R.A. 1997, ApJ, 487, 424
 Tsirropoula, G. 2000, New Astronomy, 5, 1
 Wang, H., Tang, F., Zirin, H., & Wang, J. 1996, Solar Phys. , 165, 223